

— Doctor Thesis —

Molecular mechanisms of
nutrient-stress adaptation in
Arabidopsis thaliana

(シロイヌナズナの栄養ストレス適応の分子機構)

Ichiro Kasajima

Declaration

The work described in this thesis was carried out between April, 2002 and December, 2007 under the supervision on Dr. T. Fujiwara. The work is my own except where otherwise stated in the text. The results of the first chapter were also submitted for the master degree obtained in March, 2005.

A handwritten signature in black ink, appearing to read 'I. Kasajima', with a horizontal line underneath.

Ichiro Kasajima

Contents

Summary	...	1
General Introduction	...	3
Chapter 1. The <i>BIG</i> gene is involved in regulation of sulfur deficiency-responsive genes in <i>Arabidopsis thaliana</i>		
Abbreviations	...	5
Introduction	...	5
Results	...	7
Discussion	...	11
Materials and methods	...	12
References	...	16
Figures and tables	...	18
Acknowledgements	...	25
Chapter 2. A protocol for rapid DNA extraction from <i>Arabidopsis thaliana</i> for PCR analysis		
Abbreviation	...	26
Introduction	...	26
Results and discussion	...	26
Materials and methods	...	27
References	...	29
Figure and table	...	30
Acknowledgements	...	31
Chapter 3. Identification of novel <i>Arabidopsis thaliana</i> genes which are induced by high levels of boron		
Abbreviations	...	32
Introduction	...	32
Results and discussion and methods	...	33
References	...	37
Figures and table	...	39
Acknowledgements	...	43
Chapter 4. Regulation of gene expression by boron deficiency around root tip of <i>Arabidopsis thaliana</i> and involvement of <i>WRKY6</i> in regulation		
Abbreviations	...	44

Introduction	... 44
Results	... 45
Discussion	... 48
Materials and methods	... 49
References	... 50
Figures and tables	... 52
Acknowledgements	... 59

Chapter 5. Screening of *Arabidopsis thaliana* gain-of-function mutants under nutrient deficiency

Abbreviation	... 60
Introduction	... 60
Results	... 61
Discussion	... 63
Materials and methods	... 64
References	... 65
Figures and table	... 68
Acknowledgements	... 75

Chapter 6. Differential regulation of root architecture in autotetraploid *Arabidopsis thaliana* under boron deficiency

Abbreviations	... 76
Introduction	... 76
Results	... 76
Discussion	... 79
Materials and methods	... 80
References	... 82
Figures	... 83
Acknowledgements	... 88

General Discussion

Discussion	... 89
References	... 91
Figure	... 93

Postscript	... 94
-------------------	--------

List of Figures and Tables

Chapter 1

Fig. 1-1. The <i>asr1</i> mutants	... 18
Fig. 1-2. Physiological analysis of NOB7 and <i>asr1-1</i>	... 19
Fig. 1-3. Identification of mutation in <i>asr1-1</i> and <i>asr1-2</i> mutants	... 20
Fig. 1-4. Expression of <i>GFP</i> , <i>SULTR2;2</i> , and <i>APR1</i> in <i>big-2</i>	... 21
Fig. 1-5. Effects of NPA and IAA application on the expression of <i>GFP</i> , <i>SULTR2;2</i> , and <i>APR1</i>	... 22
Fig. 1-6. Effects of IAA and NPA treatments on growth of NOB7 and <i>asr1-1</i> mutant plants	... 23
Table 1-1. Morphology of <i>asr1-1</i>	... 24
Table 1-2. Segregation of mutant phenotype in F ₂ plants	... 24
Table 1-3. Positions of T-DNA insertions in the <i>BIG</i> exon of <i>big</i> lines	... 24

Chapter 2

Fig. 2-1. Electrophoresis of PCR products	... 30
Table 2-1. Comparison of rapid methods of DNA extraction from <i>Arabidopsis</i>	... 30

Chapter 3

Fig. 3-1. The accumulated levels of B in roots and rosette leaves under various B concentrations in the growth media	... 39
Fig. 3-2. Correlation between the ratios of gene induction following B deficiency and B toxicity	... 40
Fig. 3-3. Time-course analysis of mRNA levels of <i>Arabidopsis</i> genes after exposure to low-B and high-B	... 41
Table 3-1. Induction of selected <i>Arabidopsis</i> genes by B nutrition	... 42

Chapter 4

Fig. 4-1. <i>wrky6-3</i> mutant	... 52
Fig. 4-2. Growth of <i>wrky6-3</i> mutant	... 53
Fig. 4-3. Promoter activity of <i>WRKY6</i>	... 54
Fig. 4-4. Transcriptome analysis	... 55
Table 4-1. Individual gene expressions	... 56 · 57
Table 4-2. Expressions of ACC synthases and ACC oxidases	... 58

Chapter 5

Fig. 5-1. An example of the first screening	... 68
Fig. 5-2. Growth of 'big' lines	... 69

Fig. 5-3. Cell ploidy in the shoot of big lines	... 70
Fig. 5-4. Growth of big lines on nutrient-deficient media	... 71
Fig. 5-5. Growth of F174S on media containing various concentrations of agar	... 72
Fig. 5-6. Growth of F21K	... 73
Table 5-1. Screening conditions	... 74

Chapter 6

Fig. 6-1. Growth of A119B and A142B	... 83
Fig. 6-2. Properties of A152B	... 84
Fig. 6-3. Growth of tetraploids	... 85
Fig. 6-4. Growth of tetraploids and triploids	... 86
Fig. 6-5. Growth of tetraploid under various conditions	... 87

General Discussion

Fig. D-1. Growth of activation-tagged lines	... 93
--	---------------

Summary

In this thesis I describe analysis on plant response and tolerance to nutrient deficiency with model plant *Arabidopsis thaliana*.

In the first chapter, I identified BIG as a novel sulfur response regulator. I analyzed a low-sulfur response mutant and identified mutation in the *BIG* gene. Because *BIG* is involved in auxin transport, I treated plant with indole-3-acetic acid (auxin) and *N*(1-naphthyl)phthalamic acid (auxin transport inhibitor) and these chemicals induced low-sulfur response. I also found that the patterns of gene inductions were different between *big* mutation and the chemical treatments, and concluded that the *BIG* affects low-sulfur response in an independent manner from auxin.

In the second chapter, I established a novel method for rapid DNA extraction from *Arabidopsis*. Based on reported protocols, I tried several protocols and a buffer which is the dilution of a former buffer was a successful one-step extraction buffer of DNA extraction. This method was suitable for PCR detection of T-DNA and polymorphisms between *Arabidopsis* accessions, and a small amount of sample down to 120 µg was enough for extraction.

In the third chapter, I clarified transcriptome regulation in *Arabidopsis* by boron concentrations. I performed transcriptome analysis under low-boron or high-boron conditions. Many genes were upregulated by low-boron or high-boron, and there was positive correlation between gene inductions by low-boron and high-boron conditions. High-boron induced genes were first identified in this study.

In the fourth chapter, I clarified transcriptome regulation by boron deficiency around root tip and involvement of *WRKY6* in this regulation. I performed functional analysis of low-boron or high-boron induced genes identified in the third chapter. I picked up T-DNA insertion mutants which have mutations in upregulated genes. Root elongation of one of the mutants, which has a mutation in the *WRKY6* gene, was sometimes worse than wild-type under low-boron condition. Transcript accumulation as well as promoter activity of the *WRKY6* was induced under low-boron near the root tip. In the root tip of wild-type plant grown under low-boron condition, expressions of many genes were induced. In *wrky6-3* mutant, some of these upregulated genes were not induced, suggesting the regulatory role of *WRKY6* for gene expression in the root tip under boron deficiency.

In the fifth chapter, I screened gain-of-function mutants under low-sulfur, low-boron, low-nitrogen, low-potassium, low-phosphorus, and high-boron conditions. I obtained several naturally big lines which grow bigger than wild-type under normal condition and lines showing longer root growths under boron deficiency. Because cell ploidy is a known factor which upregulate plant size, I measured cell ploidy in three naturally big lines. There was no large difference between wild-type and mutants, suggesting that some unknown factor causes bigger sizes of the isolated lines. As well as being large in size, the line named F174S was tolerant to hard gels. This phenomenon suggests the existence of some genetic mechanism for roots to

penetrate hard soils.

In the sixth chapter, I identified a novel phenotype of autotetraploid *Arabidopsis*. I further analyzed a low-boron tolerant mutant named A152B. Root elongation of this mutant was improved under boron deficiency. Because morphology of this mutant was similar to tetraploid plants, I measured cell ploidy of this mutant. Diploid cells were lacking in this mutant, confirming this mutant as tetraploid. Root elongation of other autotetraploid lines obtained from stock center was also improved under boron deficiency. Because biomass of tetraploid was not improved under boron deficiency, the observed phenotype was not identified as tolerance to boron deficiency. Taken together, differential regulation of root architecture under boron deficiency was identified as a novel phenotype of autotetraploid *Arabidopsis*.

At the end, novel methods for attaching tolerance to nutrient deficiency are indicated from recent results, and future methods for crop improvement are also discussed.

Published studies:

Chapter 1

Kasajima I, Ohkama-Ohtsu N, Ide Y, Hayashi H, Yoneyama T, Suzuki Y, Naito S, Fujiwara T (2007) The *BIG* gene is involved in regulation of sulfur deficiency-responsive genes in *Arabidopsis thaliana*. *Physiol Plant* 129: 351-363

Chapter 2

Kasajima I, Ide Y, Ohkama-Ohtsu N, Hayashi H, Yoneyama T, Fujiwara T (2004) A protocol for rapid DNA extraction from *Arabidopsis thaliana* for PCR analysis. *Plant Mol Biol Rep* 22: 49-52

Chapter 3

Kasajima I, Fujiwara T (2007) Identification of novel *Arabidopsis thaliana* genes which are induced by high levels of boron. *Plant Biotech* 24: 355-360

Other contributions (separate from the thesis):

1.

Yoneyama T, Dacanay EV, Castelo O, Kasajima I, Ho PY (2004) Estimation of soil organic carbon turnover using natural C-13 abundance in Asian tropics: A case study in the Philippines. *Soil Sci Plant Nutr* 50: 599-602

2.

Ohkama-Ohtsu N, Kasajima I, Fujiwara T, Naito S (2004) Isolation and characterization of an *Arabidopsis* mutant that overaccumulates *O*-acetyl-L-Ser. *Plant Physiol* 136: 3209-3222

General Introduction

There are seventeen essential elements for plant growth and reproduction (Cakmak and Römheld 1997). Among them, nitrogen, phosphorus, and potassium are often added to fields as fertilizers to improve crop production. This means these major nutrients are deficient in many soils. Some other nutrients (minor nutrients) are also deficient in soils, and cause agricultural problems around the world. Diverse methods have been adopted by researchers to reveal genetic mechanisms for response and tolerance to nutrient deficiency. Straight-forward screening of deficiency-sensitive loss-of-function mutant was only successful in restricted numbers of studies including identification of LKS1 which regulates AKT1 potassium transporter (Xu et al. 2006). There are also reports on identification of nutrient transporters with the use of toxic analogs, for example identification of sulfate transporter SULTR1;2 from selenate-tolerant mutants (Shibagaki et al. 2002) and identification of silicon transporters OsLsi1 and OsLsi2 from germanium-tolerant mutants (Ma et al. 2002, Ma et al. 2006, Ma et al. 2007).

Induction of expression by nutrient deficiency is also a cue to identify genes. OsPTF1, a transcription factor which improves rice growth under phosphorus deficiency was identified from its induction by phosphorus deficiency (Yi et al. 2005) and a boron transporter NIP5;1 was identified from its induction by boron deficiency (Takano et al. 2006). Several other methods were taken to identify various genes involved in the tolerance to nutrient deficiency (for only a small part of examples, Hirsch et al. 1998, Hamburger et al. 2002).

In this study, I aimed to reveal novel genetic mechanisms that improve plant tolerance to nutrient deficiency. As described above, there have been several strategies to take for this goal, and I took the same ways (chapters 1,3,4) or I also tried a novel method (chapters 5,6) in this study. In chapter 2, I established a novel high-throughput method to accelerate genetic studies. Although these extensive trials did not identify genes that improve plant tolerance to nutrient deficiency, I identified several novel aspects of plant response to nutrient deficiency. Most importantly, recent results indicate a simple method to improve plant tolerance to nutrient deficiencies through modification of functionally characterized nutrient transporters.

Cakmak I, Römheld V (1997) Boron deficiency-induced impairments of cellular functions in plants. *Plant Soil* 193: 71–83

Hamburger D, Rezzonico E, Petétot JMC, Somerville C, Poirier Y (2002) Identification and characterization of the Arabidopsis *PHO1* gene involved in phosphate loading to the xylem. *Plant Cell* 14, 889-902

Hirsch RE, Lewis BD, Spalding EP, Sussman MR (1998) A role for the AKT1 potassium channel in plant nutrition. *Science* 280: 918-921

Ma JF, Tamai K, Ichii M, Wu GF (2002) A rice mutant defective in Si uptake. *Plant Physiol* 130: 2111-2117

Ma JF, Tamai K, Yamaji N, Mitani N, Konishi S, Katsuhara M, Ishiguro M, Murata Y, Yano M (2006) A silicon transporter in rice. *Nature* 440: 688-691

Ma JF, Yamaji N, Mitani N, Tamai K, Konishi S, Fujiwara T, Katsuhara M, Yano M (2007) An efflux

- transporter of silicon in rice. *Nature* 448: 209-212
- Shibagaki N, Rose A, McDermott JP, Fujiwara T, Hayashi H, Yoneyama T, Davies JP (2002) Selenate-resistant mutants of *Arabidopsis thaliana* identify *Sultr1;2*, a sulfate transporter required for efficient transport of sulfate into roots. *Plant J* 29: 475-486
- Takano J, Wada M, Ludewig U, Schaaf G, von Wirén N, Fujiwara T (2006) The *Arabidopsis* major intrinsic protein NIP5;1 is essential for efficient boron uptake and plant development under boron limitation. *Plant Cell* 18: 1498-1509
- Xu J, Li HD, Chen L-Q, Wang Y, Liu LL, He L, Wu WH (2006) A protein kinase, interacting with two calcineurin B-like proteins, regulates K⁺ transporter AKT1 in *Arabidopsis*. *Cell* 125: 1347-1360
- Yi K, Wu Z, Zhou J, Du L, Guo L, Wu Y, Wu P (2005) OsPTF1, a novel transcription factor involved in tolerance to phosphate starvation in rice. *Plant Physiol* 138, 2087-2096

Chapter 1

The *BIG* gene is involved in regulation of sulfur deficiency-responsive genes in *Arabidopsis thaliana*

Abbreviations

APR, adenosine-5'-phosphosulfate reductase; BAC, bacterial artificial chromosome; β SR, sulfur-responsive β element; CaMV, cauliflower mosaic virus; CAPS, cleaved amplified polymorphic sequence; γ -EC, γ -glutamylcysteine; GC-MS, gas chromatography-mass spectrometry; GFP, green fluorescent protein; HPLC, high performance liquid chromatography; *Ler*, Landsberg *erecta*; NIT3, nitrilase 3; NPA, *N*-(1-naphthyl)phthalamic acid; OAS, *O*-acetyl-L-serine; ODS, octadecylsilane; ORF, open reading frame; qPCR, quantitative polymerase chain reaction; SLP, simple sequence length polymorphism; SULTR, sulfate transporter; -Sup, sulfur deficiency-induced; T-DNA, transfer DNA

Introduction

Sulfur is an essential element for higher plants. In response to sulfur deficiency, *Arabidopsis thaliana* increases the expression of the sulfate transporter genes *sulfate transporter 1:1* (*SULTR1:1*), *SULTR1:2*, *SULTR1:3*, *SULTR2:1*, *SULTR2:2*, *SULTR4:1*, and *SULTR4:2* to activate sulfate uptake and distribution (Takahashi et al. 1997, Shibagaki et al. 2002, Yoshimoto et al. 2002, 2003, Kataoka et al. 2004). The expression of genes involved in the sulfur assimilation pathway is also upregulated under conditions of sulfur deficiency. For example, the expression of *adenosine-5'-phosphosulfate reductase 1* (*APR1*), one of the *APR* gene family members in *Arabidopsis*, is induced under sulfur deficiency (Takahashi et al. 1997). Micro- and macroarray experiments have revealed hundreds of up- or downregulated genes under sulfur-deficient conditions (Hirai et al. 2003, 2004, Maruyama-Nakashita et al. 2003, Nikiforova et al. 2003). Thus, under sulfur-deficient conditions, plant growth is maintained by the regulation of a number of sulfur-responsive genes. In this chapter, genes whose mRNA accumulation is elevated under -S condition are referred to as -S_{up} genes.

Studies of two *Arabidopsis* mutants, *methionine high accumulation 1* (*mto1*) and *selenate-resistant 1* (*sel1*) support the involvement of sulfur assimilation pathway metabolites in

the regulation of several $\cdot S_{up}$ genes. The *mto1* and *sel1* mutants have mutations in the *MTO1* gene encoding cystathionine γ -synthase, a key enzyme for methionine biosynthesis (Chiba et al. 1999), and *SULTR1;2*, which encodes a sulfate transporter required for efficient sulfate uptake into the roots (Shibagaki et al. 2002), respectively. In *mto1*, the accumulation of free methionine is elevated as a result of the stabilization of *cystathionine γ -synthase* mRNA, and the expression of the β subunit gene of β -conglycinin, a soybean $\cdot S_{up}$ gene, is repressed (Hirai et al. 1994, Chiba et al. 1999). In *sel1*, the expression of *SULTR2;2*, another sulfate transporter gene, is elevated (Shibagaki et al. 2002). Transcriptome analysis revealed that the expression of a number of $\cdot S_{up}$ genes is altered in *sel1* (Maruyama-Nakashita et al. 2003). These examples support the importance of sulfur uptake and metabolism in the regulation of $\cdot S_{up}$ genes.

Forward genetics approaches have also revealed genes required for the response to phosphate deficiency. *PHR1* was isolated from a mutant in which phosphate-starvation responsive *AtIPS1::GUS* reporter activity was weakened (Rubio et al. 2001). *PHR1* (*Phosphate Starvation Response 1*) is a novel MYB family transcription factor and required for *IPS1* transcript accumulation and anthocyanin accumulation under phosphate starvation. In a related screening, another phosphate response gene *PHF1* (*Phosphate Transporter Traffic Facilitator 1*) was isolated (González et al. 2005). In *phf1* mutant, *AtIPS1::GUS* reporter activity was observed even on media with sufficient phosphate supply. The *PHF1* gene encodes a plant specific protein structurally related to the SEC12 proteins of the early secretory pathway. Without PHF1, plasma membrane phosphate transporter PHT1;1 is retained in the endoplasmic reticulum. As a result, phosphate uptake is reduced and a number of phosphate-starvation responsive genes are constitutively expressed in the mutant. Additionally, the mutant is resistant to arsenate.

Although the induction of $\cdot S_{up}$ genes has been analyzed physiologically, the molecular mechanism of their upregulation remains unknown. Recently, a *cis*-acting element of the sulfur deficiency response was identified (Maruyama-Nakashita et al. 2005). To further examine the regulation of the sulfur-deficiency response, a molecular genetic approach is taken in our laboratory. First generated was transgenic *Arabidopsis* carrying a reporter gene that responds to sulfate levels. The Naoko Ohkama Beta (NOB) lines are transgenic *Arabidopsis* that express the *green fluorescent protein* gene (*GFP*) under the control of a sulfur deficiency-responsive promoter containing the β_{SR} fragment. GFP fluorescence is enhanced in the leaves and roots of the NOB lines under conditions of sulfur deficiency unlike the NOC line which expresses *GFP* under control of the cauliflower mosaic virus 35S promoter (Ohkama et al. 2002a). The NOB7 line is an NOB line with two copies of the transgene at a single locus. From the ethylmethanesulfonate-mutagenized second-generation mutant (M_2) plants of the NOB7 line, several mutants were isolated by Dr. Naoko Ohkama-Ohtsu, in which the GFP expression level was different from that of the original NOB7 line. The *OAS high accumulation 1* (*osh1*) mutant was among them. The expression of selected $\cdot S_{up}$ genes in the mutant was elevated even at a normal sulfur concentration. The accumulation of high levels of *O*-acetyl-L-serine (OAS) in the mutant is the likely cause of the high $\cdot S_{up}$ gene expression. The *OSH1* gene was found to encode

a thiol reductase, a novel gene that regulates OAS accumulation (Ohkama-Ohtsu et al. 2004). In this chapter, I analyzed novel mutants from this screening.

Results

Characterization of mutants

Two lines of NOB7 mutants (*asr1-1* and *asr1-2*) were isolated by Dr. Ohkama as lines with high GFP expression when grown in both the medium containing 1,500 μ M sulfate (referred to as +S medium or +S condition) and the medium containing 15 μ M sulfate (referred to as -S medium or -S condition). The mutants also exhibited similar morphology: reduced expansion of rosette leaves (Fig. 1-1A), reduced lateral root formation, and reduced lengths of inflorescence shoots and siliques (Fig. 1-1B). The morphology of *asr1* was more closely analyzed. After vertical cultivation on +S medium for 11 days, the lengths of the main roots and the number of visible lateral roots of the original NOB7 and the *asr1-1* mutant were measured (Table 1-1). The average root length of *asr1-1* was 71% of that of the NOB7 plants. NOB7 had an average of 15 lateral roots, whereas *asr1-1* had only 1 lateral root on the average. The morphologies of the aerial portions of *asr1-1* and the original NOB7 were observed in detail after growth for 48 days (Table 1-1). In *asr1-1*, the inflorescence length was shorter than that in the original NOB7; there were fewer inflorescences and fewer siliques, and a greater number of cauline and rosette leaves in *asr1-1* than that in the original NOB7.

For the genetic analysis, lines were backcrossed with NOB7. The GFP fluorescence of F₁ plants grown in +S medium was similar to that of the original NOB7 line. The GFP fluorescence of individual plants of the self-pollinated F₂ generation was scored (Table 1-2). The segregation of the strength of GFP fluorescence was not significantly different from the 3:1 segregation, suggesting that each line carried a single recessive mutation responsible for the phenotype. The lines were also crossed with each other to test allelism. In this cross, the heterozygous *asr1-1* was used as the female parent because the pollination of the homozygous mutants was poor. The *asr1-1* female parent was pollinated with the homozygous *asr1-2*. If *asr1-1* and *asr1-2* were allelic mutants, the mutant and wild-type phenotypes would segregate at a 1:1 ratio. About one-half of the resulting F₁ plants showed mutant-like morphology and high GFP fluorescence, suggesting that these mutant lines were allelic to each other. The lines were named *altered sulfur response 1-1* (*asr1-1*) and *asr1-2*. The *asr1-1* and *asr1-2* mutants were backcrossed twice with NOB7 for use in the subsequent studies.

Elevation of *APR1* mRNA accumulation in *asr1*

The high GFP fluorescence levels in *asr1-1* and *-2* suggest that the sulfur deficiency-responsive promoter was induced in the mutants under +S condition. To examine whether the mutation affected the expression of endogenous -S_{up} gene, I determined the transcript levels of *SULTR2:2*

and *APR1*. *SULTR2;2* (or *AST56*) and *APR1* are among three first identified sulfur-deficiency response genes in the shoot of *Arabidopsis* (Takahashi et al. 1997). Expression of the other gene *SAT1* was not altered under -S in my experiment. The original NOB7 and *asr1-1* were grown for 10 days on +S medium, then transferred onto +S medium or -S medium, and incubated for an additional 4 days. RNA was extracted from the aerial portions of the plants and subjected to reverse transcription-mediated quantitative polymerase chain reaction analysis (Fig. 1-2A). The accumulation of *GFP*, *SULTR2;2*, and *APR1* transcripts was greater in *asr1-1* than in the original NOB7 under the +S condition. *GFP* and *APR1* expression under the -S condition was also significantly higher in *asr1-1* than the original NOB7. *SULTR2;2* transcript accumulation was on the average higher in the mutant but the difference was not significant under this -S condition.

Concentrations of sulfate, nitrate, OAS, Cys, γ -EC, and GSH in *asr1*

An easily imaginable cause of the induction of β SR-driven *GFP* and *APR1* genes in *asr1* is a change in internal metabolite concentrations. I examined the concentrations of sulfate, nitrate, OAS, cysteine (Cys), γ -glutamylcysteine (γ -EC), and glutathione (GSH) in *asr1-1*. NOB7 and *asr1-1* were grown on +S medium for 10 days, then transferred to +S or -S medium, and incubated for an additional 4 days. Sulfate concentrations in *asr1-1* were not significantly different from those in the original NOB7 under both +S and -S conditions (Fig. 1-2B). Nitrate concentrations in *asr1-1* were reduced to about 68 and 55% of those in the original NOB7 plants under +S and -S conditions, respectively (Fig. 1-2C). The concentration of OAS was lower in *asr1-1* than in NOB7 under the +S condition (about 32% of that in the original NOB7), whereas no significant difference in the OAS concentration was observed under the -S condition (Fig. 1-2D). The concentrations of Cys, γ -EC, and GSH did not differ significantly (Fig. 1-2E-G).

***asr1* mutants carry nonsense mutations in the *BIG* gene**

Rough mapping in collaboration with Dr. Ohkama revealed that the *ASR1* locus is on the upper arm of chromosome III (Fig. 1-3A). Using 1,248 lines of F₂ plants and six newly generated markers (FP55, FP27, FP2, FB9, FB27, and FB60; see Materials and methods), the *ASR1* locus was mapped to a 52,950-bp region between FP55, which is the deletion mutation of *Ler* at the 419,484th base of chromosome III, and FP2, which is the single nucleotide polymorphism between Col-0 and *Ler* at the 472,434th base of chromosome III. Based on gene predictions included in The Arabidopsis Information Resource database (<http://www.arabidopsis.org>), this region contained nine predicted genes: *At3g02250*, *At3g02260*, *At3g02270*, *At3g02280*, *At3g02290*, *At3g02300*, *At3g02310*, *At3g02315*, and *At3g02320*. Among the nine, *At3g02260* corresponded to the locus of *BIG*, a gene encoding a calossin-like protein necessary for the polar transport of the plant hormone auxin (Ruegger et al. 1997, Gil et al. 2001).

There have been many *BIG* gene mutations reported to date, e.g., *dark overexpression of CAB 1-1* (*doc1-1*), *doc1-2*, *doc1-3*, *transport inhibitor response 3-1* (*tir3-1*), *tir3-2* (Li et al. 1994, Ruegger et al. 1997, Gil et al. 2001), *umbrella 1* (*umb1*), *attenuated shade avoidance 1* (*asa1*)

(Kanyuka et al. 2003), *gibberellin 6 (ga6)* (Sponsel et al. 1997), *low phosphate-resistant root 1 (lpr1)* (López-Bucio et al. 2005), and *corymbosa 1-1 (crm1-1)* (Yamaguchi et al. 2007). Other *big* alleles have also been isolated in a mutant screening (Paciorek et al. 2005). Although the conditions used for the analyses were not identical, the morphological profiles of *asr1-1* (Table 1-2) and of the reported *big* mutants were similar in terms of decreased inflorescence height, fewer lateral roots, and a greater number of inflorescences.

The DNA sequences of the *BIG* open reading frames (ORFs; from base 428,889 to 449,888 on chromosome III) in the *asr1-1* and *asr1-2* mutants were determined. An independent single nucleotide substitution was identified in each mutant (Fig. 1-3B). Two different mRNA sequences had been predicted for *BIG* (Gil et al. 2001, Kanyuka et al. 2003). Based on the most recent report, the gene contains 14 exons and encodes a protein consisting of 5,098 amino acid residues. The following descriptions are based on the cDNA prediction by Kanyuka et al. (2003). In *asr1-1*, a C to T transition was found in exon 12 of the *BIG* gene, changing the 4504th codon of the *BIG* ORF from glutamine (CAG) to a stop codon (TAG). In *asr1-2*, a C to T transition was found in exon 14, changing the 4876th codon, also a glutamine (CAA), to a stop codon (TAA). These nonsense mutations in *asr1-1* and *asr1-2*, together with the mutations in *doc1-1*, *doc1-2*, *doc1-3*, *tir3-1*, *tir3-2*, *umb1*, and *asa1*, are shown in Fig. 1-3B.

Genetic analysis of T-DNA insertion mutants in the *BIG* gene

T-DNA insertion mutants of the *BIG* gene were established and termed as *big-1*, *big-2*, *big-3*, and *big-4*. The accumulation of *BIG* mRNA was greatly reduced or was not detected in these mutants. Because the homozygous female parent was poorly fertile, each homozygous mutant was crossed with a heterozygous *asr1-1* female parent, and the F₁ plants from these crosses were grown in the greenhouse. Visible phenotypes of the *asr1-1* mutant, such as reduced apical dominance and reduced lateral root formation, were observed in about the half of the F₁ plants from every cross, indicating that the lesion in the *BIG* gene caused the *big*-like morphology in *asr1-1*.

I also tested whether the T-DNA insertion mutations in the *BIG* gene induced the expression of β SR-driven *GFP* and *APR1* genes. To examine the effect of the *big-2* mutation on the activity of the promoter containing the β SR fragment, the *big-2* mutant was crossed with the *asr1-1* heterozygous mutant. From the F₂ progeny, a line that was homozygous for the *big-2* mutation and homozygous for the NOB7 T-DNA insertion was selected by PCR and named *big-2* (NOB7). The seeds of *big-2* (NOB7) were sown on +S medium together with seeds of NOB7 and NOC2. After incubation for 10 days, the plants were transferred to +S or -S medium and incubated for another 4 days. The GFP fluorescence of these plants was observed (Fig. 1-4A) and quantified for individual plants (Fig. 1-4B). The GFP fluorescence of *big-2* (NOB7) was higher than that of the original NOB7 under both +S and -S conditions, and it was induced by -S.

The expressions of *SULTR2;2* and *APR1* were analyzed in *big-2* after cultivation on +S and -S medium as described above. RNA was extracted from the aerial portions, and the accumulations of *SULTR2;2* and *APR1* transcripts were measured (Fig. 1-4C). The mRNA

accumulation of *APR1* was higher in the aerial portions of *big-2* than in the aerial portions of the wild type. mRNA accumulation of *SULTR2;2* was not altered under both sulfur conditions.

Effects of auxin and an auxin transport inhibitor on gene expression

As BIG is involved in the regulation of the polar transport of auxin (Gil et al. 2001), auxin metabolism may likely to regulate β_{SR} -driven *GFP* in *big* mutant. I examined the effects of auxin and a polar auxin transport inhibitor on β_{SR} -driven *GFP*, *SULTR2;2* and *APR1* gene expressions. I first tested *N*-(1-naphthyl)phthalamic acid (NPA), an inhibitor of polar auxin transport. NOB7 and *asr1-1* were cultivated on normal medium or medium containing 10 μ M NPA, and the GFP fluorescence intensity was observed (Fig. 1-5A,B). The GFP fluorescence intensity and the accumulation of *GFP* transcripts (Fig. 1-5C) were dramatically elevated by the application of NPA in both NOB7 and *asr1-1*. This induction of gene expression was prominent in NPA-treated *asr1-1*. The effect of indole-3-acetic acid (IAA) was also tested. Both *asr1-1* and NOB7 were grown for 10 days on normal medium and transferred to normal medium with or without 10 μ M IAA. After 4 days of incubation, GFP fluorescence was examined (Fig. 1-5D). Both *asr1-1* and the original NOB7 showed an elevated level of GFP fluorescence in response to the IAA treatment (Fig. 1-5D,E). The accumulation of mRNA transcripts of these genes in IAA-treated plants was also examined (Fig. 1-5F). In the aerial portions of IAA-treated NOB7, the expression levels of *GFP* and *SULTR2;2* were markedly higher than those in the control.

Growth inhibition by auxin and an auxin transport inhibitor

To investigate the effects of the long-term application of auxin or an auxin transport inhibitor on the growth of wild-type and mutant plants, *asr1-1* and the original NOB7 were grown on normal medium or medium containing 10 μ M IAA (Fig. 1-6A). In the absence of IAA, the petioles of *asr1-1* were shorter than those of the original NOB7, and leaf color was not obviously different between the two. In the presence of 10 μ M IAA, rosette leaf expansion was inhibited and the rosette leaves were pale green in the original NOB7. In *asr1-1* cultivated with 10 μ M IAA, the expansion of the rosette leaves was strongly reduced, producing leaves about one-third the length of NOB7 leaves, and the green color of the rosette leaves was nearly lost in *asr1-1*. Some leaves turned purple in *asr1-1* plants, probably as a result of anthocyanin accumulation. Thus, the *asr1* mutant is more sensitive to excess IAA than the original NOB7.

The growth of *asr1-1* and the original NOB7 was also tested on medium containing 10 μ M NPA (Fig. 1-6B). NPA inhibited root elongation in NOB7, but shoot size was not greatly reduced. In *asr1-1*, elongation of the primary root was not strongly inhibited by NPA, as was observed for other *big* mutants. However, NPA markedly reduced shoot size in *asr1-1*.

Discussion

In this chapter, *asr1* mutants were analyzed that express higher levels of β_{SR} -driven *GFP* under +S conditions. Subsequent analysis indicated that *ASR1* is *BIG*, but it was not clear why the loss of *BIG* gene function would induce β_{SR} -driven *GFP* expression. Changes in metabolite contents did not explain the induction of β_{SR} -driven *GFP*. In the *asr1* mutants, the concentrations of sulfate, Cys, γ -EC, and GSH, which correlate negatively with β_{SR} -driven *GFP* expression, were not notably different from those in the wild type. The concentration of OAS in the mutants was lower than that in the wild type only under the +S condition (Fig. 1-2). It is likely that *BIG* affects a signal transduction pathway independently of OAS and/or GSH. Alternatively, it is possible that *BIG* affects a signal transduction pathway downstream of OAS and GSH.

Previously reported *big* mutants had defects in a number of processes, including light-signaling pathway, sensitivity to auxin transport inhibitors, polar auxin transport, shade avoidance, cytokinin sensitivity, ethylene sensitivity, gibberellin signaling, and alterations of root architecture induced by phosphate deficiency (Li et al. 1994, Ruegger et al. 1997, Sponsel et al. 1997, Kanyuka et al. 2003, López-Bucio et al. 2005). The inhibition of polar auxin transport is a well-characterized aspect of *big* mutants (Gil et al. 2001). The binding of NPA to microsomal membranes is reduced in a *big* mutant (Ruegger et al. 1997), and the extent of pin-formed 1 (PIN1) mislocalization resulting from NPA application is elevated in *big* mutants (Gil et al. 2001). A recent report showed that *BIG* is required for the inhibitory effect of auxin on cellular endocytosis (Paciorek et al. 2005). These findings suggest that *BIG* regulates auxin transport via PIN recycling.

In the present study, I examined the effects of exogenously applied auxin and a polar auxin transport inhibitor on the β_{SR} -driven *GFP*. Both treatments induced β_{SR} -driven *GFP*, implying the auxin as the cause of β_{SR} -driven *GFP* induction in *big*. Genevestigator (Zimmermann et al. 2004) indicated no induction of *SULTR2;2* or *APR1* expression by IAA. This implies that IAA induction depends on detailed treatment conditions. It is noteworthy that *SULTR2;2* expression was highly elevated in auxin-treated plants unlike the case of the *big* mutants in which slight or undetectable levels of induction was observed. This difference in the pattern of *SULTR2;2* induction between auxin treatment and the *big* mutation suggest that effect of the *big* mutation is not mediated by auxin. It is more likely that β_{SR} -driven *GFP* and *APR1* inductions in *big* mutants result from one of the pleiotropic effects of the *BIG* gene which is independent of auxin.

Then, how can we understand the effect of NPA? The inhibition of polar auxin transport is likely to have an impact on the auxin concentration. Auxin transport inhibitors are thought to increase IAA accumulation in the root tip, thus inhibiting normal root growth (Muday and Haworth 1994, Muday et al. 1995). Additionally, by screening for *tir* mutants for resistance to auxin transport inhibitors, ten new alleles of *auxin resistant 1* (*axr1*) auxin-resistant mutants

were isolated (Ruegger et al. 1997), indicating that auxin transport inhibitors affect plant growth by increasing the auxin concentration in the plant body. These data suggest that the effect of auxin transport inhibition occurs through elevated levels of IAA in plant tissues. In contrast, a more recent report (Ljung et al. 2001) revealed that NPA inhibits IAA biosynthesis in expanding leaves and cotyledons.

IAA affected the growth of the *asr1* mutant more severely than that of NOB7. In the presence of NPA, shoot growth was more severely affected and root elongation was less affected in *asr1* than in NOB7. These growth patterns of *asr1* and NOB7 in response to IAA or NPA can be explained as the result of a possibly elevated concentration of IAA in the shoot of *asr1*.

It is also possible that the expression of several $-S_{up}$ genes is regulated by auxin. Kutz et al. (2002) indicated the hypothetical involvement of IAA in the regulation of root morphology under conditions of sulfur deficiency. They reported that the expression of the *Nitrilase3* (*NIT3*) gene, which encodes an enzyme that catalyzes the transformation of indole-3-acetonitrile to IAA, is enhanced in sulfur-deficient plants. The promoter activity of *NIT3* is weak in both leaves and roots during vegetative stages and is undetectable during bolting and flowering stages in plants grown in medium containing a normal concentration of sulfate. When plants are exposed to sulfur deficiency, *NIT3* expression greatly increases. Furthermore, Nikiforova et al. (2003) showed that the expression levels of genes involved in IAA biosynthesis and IAA signaling are altered in plants under sulfur deficiency. On the other hand, expression of auxin-responsive DR5-GUS reporter gene is downregulated by sulfur deficiency, and expression of a $-S_{up}$ gene is downregulated by auxin, suggesting negative role of auxin in sulfur-deficiency response (Dan et al. 2007). Further analyses are necessary to reveal the detailed roles of BIG and IAA in the signaling pathway of sulfur deficiency.

Materials and methods

Plant materials and chemicals

Two transgenic lines of *Arabidopsis thaliana* (L.) Heynh. ecotype Col-0, NOB7 and NOC2 (Ohkama et al. 2002a), and T-DNA insertion lines from the Salk Institute (La Jolla, CA, USA) were used in this study. The line NOB7 carries a chimeric promoter driving *GFP* (*Pro35S:: β SRx3::GFP*). The NOC2 line carries the *GFP* ORF under the control of the cauliflower mosaic virus (CaMV) 35S RNA promoter (*Pro35S::GFP*) and was used as a control. The T-DNA insertion lines have T-DNA insertions in the exon regions of the *BIG* gene. IAA was obtained from ICN Biomedicals (Aurora, OH, USA). *N*-(1-naphthyl)phthalamic acid was obtained from Frinton Laboratories (Vineland, NJ, USA).

Plant culture conditions

Surface-sterilized seeds were sown on sterilized growth medium (Hirai et al. 1995) containing

1% (w/v) sucrose and 0.8% (w/v) agar (Wako, Osaka, Japan). The seeds were incubated on culture plates at 4°C for 4 days and were then grown at 22°C under fluorescent lamps with a 16-h light/8-h dark cycle. The plates were placed vertically in the growth chamber to allow the roots to grow on the surface of the medium. The concentrations of sulfate in the culture medium were adjusted by replacing magnesium sulfate with an equimolar amount of magnesium chloride. For the morphological analysis of mature plants, the plants were grown in the greenhouse at 22°C under fluorescent lamps with a 16-h light/8-h dark cycle.

Analysis of *GFP* expression using a quantitative fluorescence imaging system

GFP activity was determined using a quantitative fluorescence imaging system as described previously (Niwa et al. 1999). Plants were scanned with an argon laser (488 nm), and the GFP fluorescence (530 nm) and chlorophyll auto-fluorescence (610 nm) were detected and synthesized using ImageQuant software (Molecular Dynamics, Sunnyvale, CA, USA).

Map-based cloning of the *ASR1* locus

The *ASR1* locus was identified in collaboration with Dr. Ohkama using co-dominant PCR markers. For the rough map-based cloning, markers nga63, ciw12, nga280, nga111, ciw2, nga168, nga162, ciw4, nga8, ciw6, nga1107, CTR1, and ciw10 were used. For the fine mapping, primers were generated to amplify the sites of polymorphism between the ecotype Col-0 and *Ler*. About 30 sets of primers were generated and used as simple sequence-length polymorphism, cleaved amplified polymorphic sequence, or other types of PCR markers. Successful markers were selected, and the DNA samples from recombined F₂ plants were analyzed. Six primer sets (FP55, FP27, FP2, FB9, FB27, and FB60) were used to test the samples for the fine mapping. The primer set FP55 (5'-TAA TCC GGG TTA TGG GAT CA-3' / 5'-GCC TCT CAG ATT AAA AGA TGG A-3') was used to amplify the 55,403rd base position of F14P3 (GenBank Accession No. AC009755), giving a 118-bp PCR product from Col-0 genomic DNA and a 98-bp PCR product from *Ler* genomic DNA. The PCR products were subjected to electrophoresis in a 4% Nusieve 3:1 agarose gel (Takara, Kyoto, Japan). The primer sets FP27 (5'-CCA GTT GAC CGG CTT CTT AT-3' / 5'-GAC AAA CAC AGC GAA GGT GA-3') and FP2 (5'-TTG CAA TCC TGC TTC ACA AC-3' / 5'-ATC CAC TGC ATC CCT TAG GA-3') were used to amplify the 27,781st and 2,454th bases of F14P3, respectively, and the PCR products were sequenced to detect the single nucleotide polymorphisms between the Col-0 and *Ler* ecotypes at each position. The primer sets FB9 (5'-TGA ACC AAA GAC AGG GGA TT-3' / 5'-CTT GGG GTT CTC TCT TGG G-3') and FB60 (5'-AAC TCG GAC CAG ACT CGT GA-3' / 5'-AAT TGG ATC GGA TTC ACT CG-3') were used to amplify the 9,340th and 60,960th bases, respectively, of F16B3 (GenBank Accession No. AC021640). The FB9 PCR product was digested with *AseI* to specifically digest the PCR product from *Ler* genomic DNA, and the FB60 PCR product was digested with *ClaI* to specifically digest the PCR product from Col-0 genomic DNA. The primer set FB27 (5'-TCT TAA TCT TTT TAT TTC CGA TGA CA-3' and 5'-TCA AAA GTC CAC TTC TCC CTT T-3') was used to amplify the 27,367th base of F16B3, producing a 144-bp product from Col-0 genomic DNA

and a 139-bp product from *Ler* genomic DNA. The PCR products were subjected to electrophoresis in an 8.4% polyacrylamide gel. Genomic DNA was extracted using a DNeasy plant kit (Qiagen K.K., Tokyo, Japan).

Quantification of mRNA accumulation by qPCR

Total RNA was extracted and simultaneously treated with DNase using an RNeasy plant mini kit and RNase-free DNase set (Qiagen K.K.) as recommended by the manufacturer. RNA was reverse transcribed using MuLV reverse transcriptase (Applied Biosystems, Foster City, CA, USA) and an oligo-d(T)₁₆ primer. The cDNA was amplified by PCR in a SmartCycler (Cepheid, Sunnyvale, CA, USA) with Ex-Taq R-PCR Version (Takara). I calculated the relative amounts of mRNA, using serial dilutions of a concentrated first-strand cDNA stock solution. The primer sets for quantitative polymerase chain reactin (qPCR) were 5'-CAT TGG AGC CAA AAG TTT CGC-3' and 5'-TCC TCA ATC TCA ACC ACA TCA AC-3' for *APR1* and 5'-CGA CAT GTC TTG CGT GAT GGG CG-3' and 5'-GCT CGC TTC AAT TTG TGA AGT ACC CT-3' for *SULTR2;2*, as described (Ohkama et al. 2002b). The other primers used were: 5'-CAC ATG AAG CAG CAC GAC TT-3' and 5'-AGT TCA CCT TGA TGC CGT TC-3' for *GFP*, 5'-GCC AGA TCT TCA TCG TCG TG-3' and 5'-TCT CCA GCG AAT CCA ACC TT-3' for *Actin8Q*, 5'-GCC AGA TCT TCA TCG TCG TG-3' and 5'-TCT CCA GCG AAT CCA ACC TT-3' for β -*Tubulin*, and 5'-CCT TGG TGT CAA GCA GAT GA-3' and 5'-TGAAGA CAC CTC CTT GAT GAT TT-3' for *Elongation Factor 1a*.

Measurement of the metabolite contents of the shoot

Plants were grown for 10 days on medium (Hirai et al. 1994) containing 1,500 μ M sulfate (+S medium or +S condition) and then transferred to +S medium or to medium containing 15 μ M sulfate (-S medium or -S condition) for 4 days. The plant shoots were collected and initially powdered with liquid nitrogen, and each metabolite was extracted. The measurement of thiol compounds followed a previously described procedure (Ohkama et al. 2002a). Thiol compounds were extracted with 80% ethanol at 65°C and were measured by high performance liquid chromatography (HPLC). The extraction and analysis of OAS were performed as described by Kim et al. (1999). The anion concentrations were determined using an HP^{3D} capillary electrophoresis system and an HP Inorganic Anion Analysis kit (Hewlett Packard, Wilmington, DE, USA).

Observation of plant morphology

After vernalization, the original NOB7 and *asr1-1* plants were cultivated vertically for 11 days on +S medium (Hirai et al. 1994). The root morphology was examined in these plants. Root length was analyzed by measuring the distance from the shoot-root junction to the root tip on the medium, and the number of lateral roots longer than or equal to 1 mm was counted.

After vernalization, NOB7 and *asr1-1* were cultivated vertically for 2 weeks on +S medium, then transferred onto rock-wool on vermiculite, and cultivated for 32 days to examine the shoot morphology. Height was measured as the distance from the shoot-root junction to the

top of the first inflorescence. The numbers of the following were counted: inflorescences (1 cm or longer); siliques, including immature siliques; cauline leaves (4 mm or longer), containing petioles; and rosette leaves (4 mm or longer).

Establishment of T-DNA insertion mutants

The lines *big-1* (SALK_105495), *big-2* (SALK_045560), *big-3* (SALK_107817), and *big-4* (SALK_015237) had T-DNA insertions in exons 10, 5, 4, and 3 of the *BIG* gene, respectively, according to the T-DNA flanking sequence obtained from the Salk Institute Web site (<http://signal.salk.edu/>).

T-DNA inserted lines (Alonso et al. 2003) were provided from the Arabidopsis Biological Resource Center, and primers for detecting T-DNA insertions in each of the four lines were designed according to the protocol on the Salk Institute Web site. For each mutant, the DNA sequences around the left and/or right borders of the T-DNA insertion were determined (Table 1-3). As predicted in the database, each genomic sequence flanking the pROK2 (Alonso et al. 2003) T-DNA border sequences was found in the exon regions of the *BIG* gene.

Primers were generated for identifying the T-DNA insertions in the *big* mutants. The DNA sequences of the primers were: 5'-CCA CCA TAT TCT CGA ACT GCA CC-3' and 5'-ACT GCA AAC CCA TGC AGA GGA-3' for SALK_105495 (*big-1*), 5'-CCA TTC ATC TCC AGA AAG ACG GA-3' and 5'-TCT GTC TCC AAT CCA AAC CCT GA-3' for SALK_045560 (*big-2*), 5'-CTG CCT TTT TCC CCT TCC ACA-3' and 5'-GAA GAC AAG GCT TCT GAT GGT GG-3' for SALK_107817 (*big-3*), 5'-CCC TCT GTA GCA GTG TGG TTA GTG A-3' and 5'-TTG TTT TTC GAT GAT GAT TAG ACG TTT G-3' for SALK_015237 (*big-4*). These primers were used with 5'-GCG TGG ACC GCT TGC TGC AAC T-3' (LBb1) or 5'-TGG TTC ACG TAG TGG GCC ATC G-3' (LbA1) in the PCR reaction mixture, as described on the SIGnAL Web page (<http://signal.salk.edu/tdnaprimers.html>). DNA samples were prepared as described in chapter 2 (Kasajima et al. 2004).

DNA sequence determination of the *BIG* gene region

The target of the DNA sequencing was from the 25,000th to the 46,000th base of F14P3 (GenBank Accession No. AC009755), which contains the *BIG* ORF and promoter region. About 50 pairs of primers were designed to amplify DNA fragments of about 500 bp. The sequence analysis was performed using an ABI PRISM 310 (Perkin-Elmer Japan, Chiba, Japan) as recommended by the manufacturer.

References

- Alonso JM, Stepanova AN, Leisse TJ, Kim CJ, Chen H, Shinn P, Stevenson DK, Zimmerman J, Barajas P, Cheuk R, Gadrinab C, Heller C, Jeske A, Koesema E, Meyers CC, Parker H, Prednis L, Ansari Y, Choy N, Deen H, Geralt M, Hazari N, Hom E, Karnes M, Mulholland C, Ndubaku R, Schmidt I, Guzman P, Aguilar-Henonin L, Schmid M, Weigel D, Carter DE, Marchand T, Risseuw E, Brogden D, Zeko A, Crosby WL, Berry CC, Ecker JR (2003) Genome-wide insertional mutagenesis of *Arabidopsis thaliana*. *Science* 301: 653-657
- Chiba Y, Ishikawa M, Kijima F, Tyson RH, Kim J, Yamamoto A, Nambara E, Leustek T, Wallsgrove RM, Naito S (1999) Evidence for autoregulation of cystathionine γ -synthase mRNA stability in *Arabidopsis*. *Science* 286: 1371-1374
- Dan H, Yang G, Zheng Z-L (2007) A negative regulatory role for auxin in sulphate deficiency response in *Arabidopsis thaliana*. *Plant Mol Biol* 63: 221-235
- Gil P, Dewey E, Friml J, Zhao U, Snowden KC, Putterill J, Palme K, Estelle M, Chory J (2001) BIG: a calossin-like protein required for polar auxin transport in *Arabidopsis*. *Genes Dev* 15: 1985-1997
- González E, Solano R, Rubio V, Leyva A, Paz-Ares J (2005) PHOSPHATE TRANSPORTER TRAFFIC FACILITATOR1 is a plant-specific SEC12-related protein that enables the endoplasmic reticulum exit of a high-affinity phosphate transporter in *Arabidopsis*. *Plant Cell* 17: 3500-3512
- Hirai MY, Fujiwara T, Goto K, Komeda Y, Chino M, Naito S (1994) Differential regulation of soybean seed storage protein gene promoter-GUS fusions by exogenously applied methionine in transgenic *Arabidopsis thaliana*. *Plant Cell Physiol* 35: 927-934
- Hirai MY, Fujiwara T, Chino M, Naito S (1995) Effects of sulfate concentrations on the expression of a soybean seed storage protein gene and its reversibility in transgenic *Arabidopsis thaliana*. *Plant Cell Physiol* 36: 1331-1339
- Hirai MY, Fujiwara T, Awazuhara M, Kimura T, Noji M, Saito K (2003) Global expression profiling of sulfur-starved *Arabidopsis* by DNA macroarray reveals the role of *O*-acetyl-L-serine as a general regulator of gene expression in response to sulfur nutrition. *Plant J* 33: 651-663
- Hirai MY, Yano M, Goodenowe DB, Kanaya S, Kimura T, Awazuhara M, Arita M, Fujiwara T, Saito K (2004) Integration of transcriptomics and metabolomics for understanding of global responses to nutritional stresses in *Arabidopsis thaliana*. *Proc Natl Acad Sci USA* 101: 10205-10210
- Kanyuka K, Praekelt U, Franklin KA, Billingham OE, Hooley R, Whitelam GC, Halliday KJ (2003) Mutations in the huge *Arabidopsis* gene *BIG* affect a range of hormone and light responses. *Plant J* 35: 57-70
- Kasajima I, Ide Y, Ohkama N, Hayashi H, Yoneyama T, Fujiwara T (2004) A protocol for rapid DNA extraction from *Arabidopsis thaliana* for PCR analysis. *Plant Mol Biol Rep* 22: 49-52
- Kataoka T, Watanabe-Takahashi A, Hayashi N, Ohnishi M, Mimura T, Buchner P, Hawkesford MJ, Yamaya T, Takahashi H (2004) Vacuolar sulfate transporters are essential determinants controlling internal distribution of sulfate in *Arabidopsis*. *Plant Cell* 16: 2693-2704
- Kim H, Hirai MY, Hayashi H, Chino M, Naito S, Fujiwara T (1999) Role of *O*-acetyl-L-serine in the coordinated regulation of the expression of a soybean seed storage-protein gene by sulfur and nitrogen nutrition. *Planta* 209: 282-289
- Kutz A, Müller A, Hennig P, Kaiser WM, Piotrowski M, Weiler EW (2002) A role for nitrilase 3 in the regulation of root morphology in sulfur-starving *Arabidopsis thaliana*. *Plant J* 30: 95-106
- Li H, Altschmied L, Chory J (1994) *Arabidopsis* mutants define downstream branches in the phototransduction pathway. *Genes Dev* 8: 339-349
- Ljung K, Bhalerao RP, Sandberg G (2001) Sites and homeostatic control of auxin biosynthesis in *Arabidopsis* during vegetative growth. *Plant J* 28: 465-474
- López-Bucio J, Hernández-Abreu E, Sánchez-Calderón L, Pérez-Torres A, Rampey RA, Bartel B, Herrera-Estrella L (2005) An auxin transport independent pathway is involved in phosphate stress-induced root architectural alterations in *Arabidopsis*. Identification of *BIG* as a mediator of auxin in pericycle cell activation. *Plant Physiol* 137: 681-691
- Maruyama-Nakashita A, Inoue E, Watanabe-Takahashi A, Yamaya T, Takahashi H (2003) Transcriptome profiling of sulfur-responsive genes in *Arabidopsis* reveals global effects of sulfur nutrition on multiple metabolic pathways. *Plant Physiol* 132: 597-605
- Maruyama-Nakashita A, Nakamura Y, Watanabe-Takahashi A, Inoue E, Yamaya T, Takahashi H (2005) Identification of a novel *cis*-acting element conferring sulfur deficiency response in *Arabidopsis* roots. *Plant J* 42: 305-314

- Muday GK, Haworth P (1994) Tomato root growth, gravitropism, and lateral development: correlation with auxin transport. *Plant Physiol Biochem* 32: 193-203
- Muday GK, Lomax TL, Rayle DL (1995) Characterization of the growth and auxin physiology of roots of the tomato mutant, *diageotropica*. *Planta* 195: 548-553
- Nikiforova V, Freitag J, Kempa S, Adamik M, Hesse H, Hoefgen R (2003) Transcriptome analysis of sulfur depletion in *Arabidopsis thaliana*: interlacing of biosynthetic pathways provides response specificity. *Plant J* 33: 633-650
- Niwa Y, Hirano T, Yoshimoto K, Shimizu M, Kobayashi H (1999) Non-invasive quantitative detection and applications of non-toxic, S65T-type green fluorescent protein in living plants. *Plant J* 18: 455-463
- Ohkama N, Goto DB, Fujiwara T, Naito S (2002a) Differential tissue-specific response to sulfate and methionine of a soybean seed storage protein promoter region in transgenic *Arabidopsis*. *Plant Cell Physiol* 43: 1266-1275
- Ohkama N, Takei K, Sakakibara H, Hayashi H, Yoneyama T, Fujiwara T (2002b) Regulation of sulfur-responsive gene expression by exogenously applied cytokinins in *Arabidopsis thaliana*. *Plant Cell Physiol* 43: 1493-1501
- Ohkama-Ohtsu N, Kasajima I, Fujiwara T, Naito S (2004) Isolation and characterization of an *Arabidopsis* mutant that overaccumulates *O*-acetyl-L-Ser. *Plant Physiol* 136: 3209-3222
- Pacioerek T, Zajímalová E, Ruthardt N, Petrášek J, Stierhof Y-D, Kleine-Vehn J, Morris DA, Emans N, Jürgens G, Geldner N, Friml J (2005) Auxin inhibits endocytosis and promotes its own efflux from cells. *Nature* 435: 1251-1256
- Rubio V, Linhares F, Solano R, Martin AC, Iglesias J, Leyva A, Paz-Ares JA (2001) Conserved MYB transcription factor involved in phosphate starvation signaling both in vascular plants and in unicellular algae. *Genes Dev* 15: 2122-2133
- Ruegger M, Dewey E, Hobbie L, Brown D, Bernasconi P, Turner J, Muday G, Estelle M (1997) Reduced naphthylphthalamic acid binding in the *tir3* mutant of *Arabidopsis* is associated with a reduction in polar auxin transport and diverse morphological defects. *Plant Cell* 9: 745-757
- Shibagaki N, Rose A, McDermott JP, Fujiwara T, Hayashi H, Yoneyama T, Davies JP (2002) Selenate-resistant mutants of *Arabidopsis thaliana* identify *Sultr1;2*, a sulfate transporter required for efficient transport of sulfate into roots. *Plant J* 29: 475-486
- Sponsel VM, Schmidt FW, Porter SG, Nakayaam M, Kohlstruck S, Estelle M (1997) Characterization of new gibberellin-responsive semidwarf mutants of *Arabidopsis*. *Plant Physiol* 115: 1009-1020
- Takahashi H, Yamazaki M, Sasakura N, Watanabe A, Leustek T, Engler JD, Engler G, Van Montagu M, Saito K (1997) Regulation of sulfur assimilation in higher plants: A sulfate transporter induced in sulfate-starved roots plays a central role in *Arabidopsis thaliana*. *Proc Natl Acad Sci USA* 94: 11102-11107
- Yamaguchi N, Suzuki M, Fukaki H, Morita-Terao M, Tasaka M, Komeda Y (2007) CRM1/BIG-mediated auxin action regulates *Arabidopsis* inflorescence development. *Plant Cell Physiol* 48: 1275-1290
- Yoshimoto N, Takahashi H, Smith FW, Yamaya T, Saito K (2002) Two distinct high-affinity sulfate transporters with different inducibilities mediate uptake of sulfate in *Arabidopsis* roots. *Plant J* 29: 465-473
- Yoshimoto N, Inoue E, Saito K, Yamaya T, Takahashi H (2003) Phloem-localizing sulfate transporter, *Sultr1;3*, mediates re-distribution of sulfur from source to sink organs in *Arabidopsis*. *Plant Physiol* 131: 1511-1517
- Zimmermann P, Hirsch-Hoffmann M, Hennig L, Gruissem W (2004) GENEVESTIGATOR. *Arabidopsis* Microarray Database and Analysis Toolbox. *Plant Physiol* 136: 2621-2632

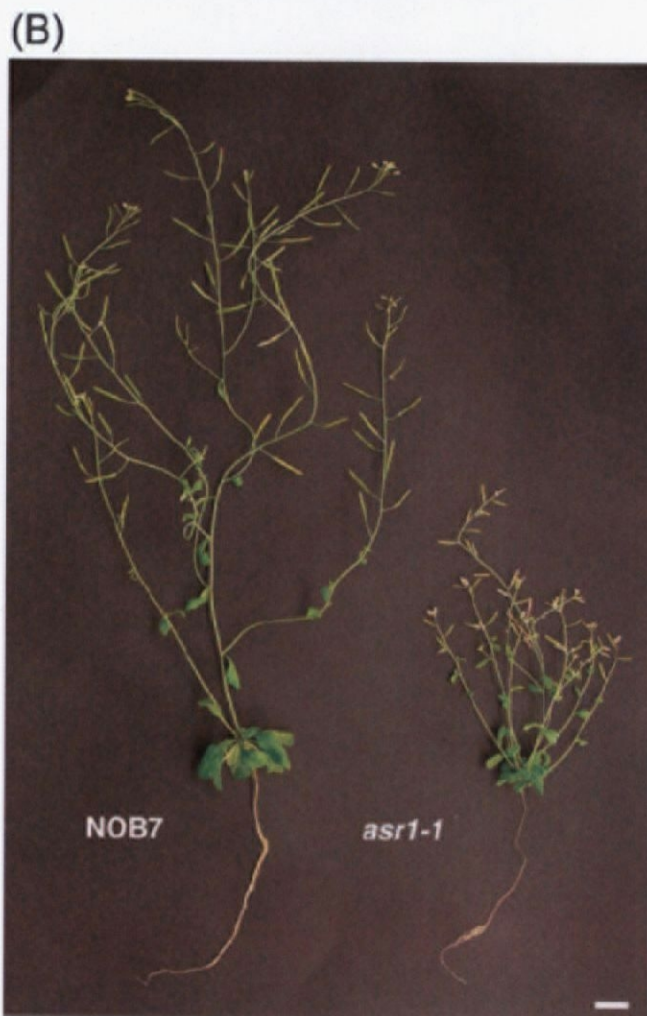


Fig. 1-1. The *asr1* mutants. (A) GFP fluorescence of *asr1* mutants. Transgenic NOC2 and NOB7 lines and two alleles of *asr1* mutants *asr1-1* and *asr1-2* were grown on the normal medium containing 1,500 μ M of sulfate for 27 days. Then plants were scanned fluorometrically. Images obtained with two filters each for GFP fluorescence and chlorophyll auto-fluorescence were colored green and red, respectively, and overlaid to generate a false image representing relative GFP intensities. Transgenic NOC2 carried *GFP* under control of the cauliflower mosaic virus 35S RNA promoter and expressed a constantly high level of GFP protein. Transgenic NOB7 carried *GFP* under control of the three repeats of β_{SR} sulfur-deficiency response promoter fused to cauliflower mosaic virus 35S RNA promoter. Bar = 1 cm. (B) Morphology of mature plants. NOB7 (left) and *asr1-1* were grown for 41 days. Bar = 1 cm.

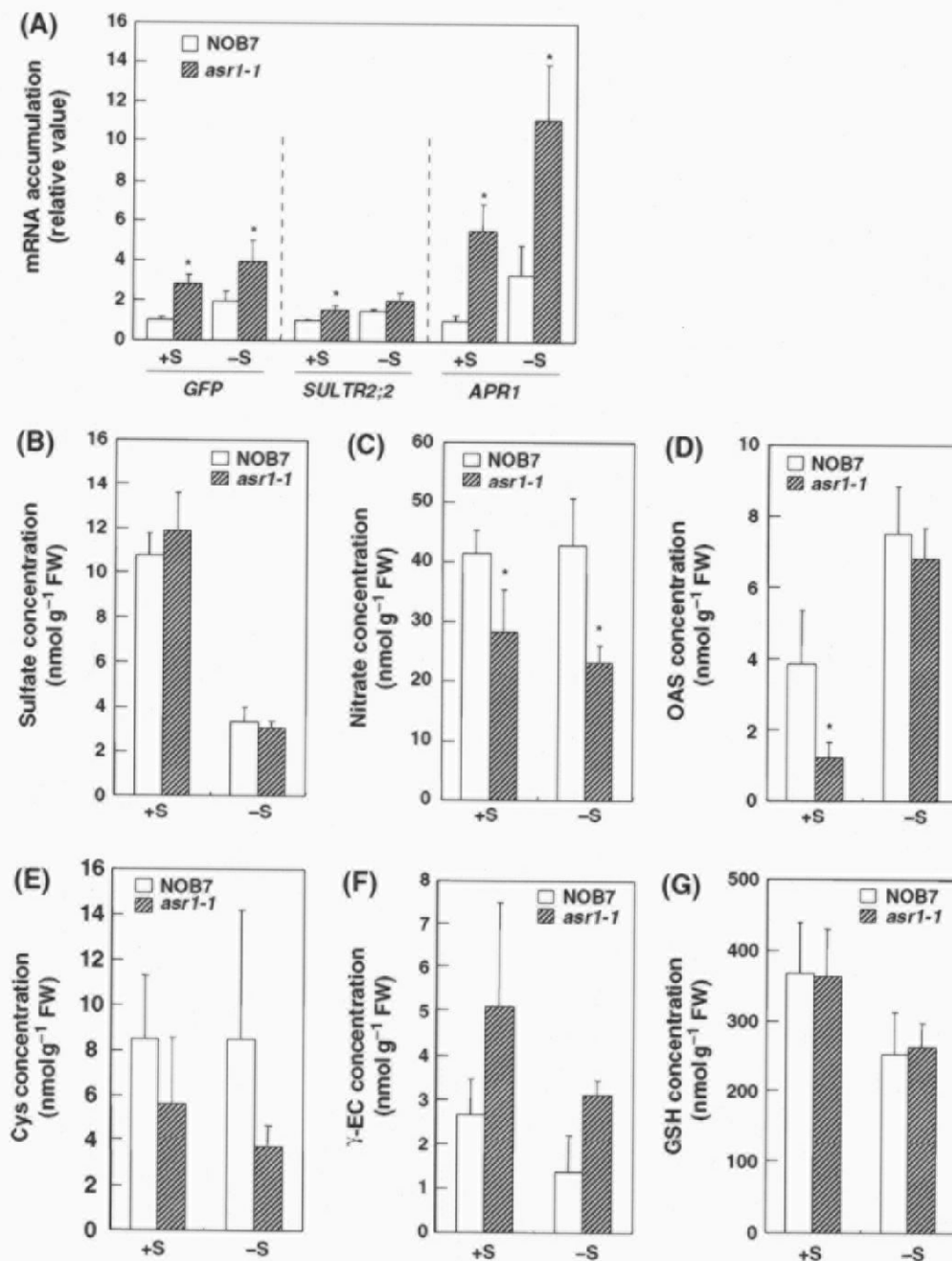


Fig. 1-2. Physiological analysis of NOB7 and *asr1-1*. (A) Quantitative polymerase chain reaction (qPCR) analysis. Ten-day-old NOB7 and *asr1-1* plants were cultivated for 4 days on the normal medium containing 1,500 μM sulfate (+S) or sulfur-deficient medium containing 15 μM sulfate (-S). Total RNA was extracted from shoots, reverse transcribed with oligo-(dT)₁₆ primer, and the resultant cDNA was subjected to qPCR analysis. Monitored genes were *GFP*, *SULTR2;2*, and *APR1*, whose mRNA accumulations were increased by sulfur deficiency; mRNA accumulation was standardized with the *Actin8Q* gene mRNA accumulation. (B)–(G) Quantitative analysis of sulfur-related metabolites. (B) Sulfate concentration. (C) Nitrate concentration. (D) OAS concentration. (E) Cysteine concentration. (F) γ-EC concentration. (G) Glutathione concentration. Asterisks indicate significant changes using Student's *t* test ($P = 0.05$, $n = 4$).

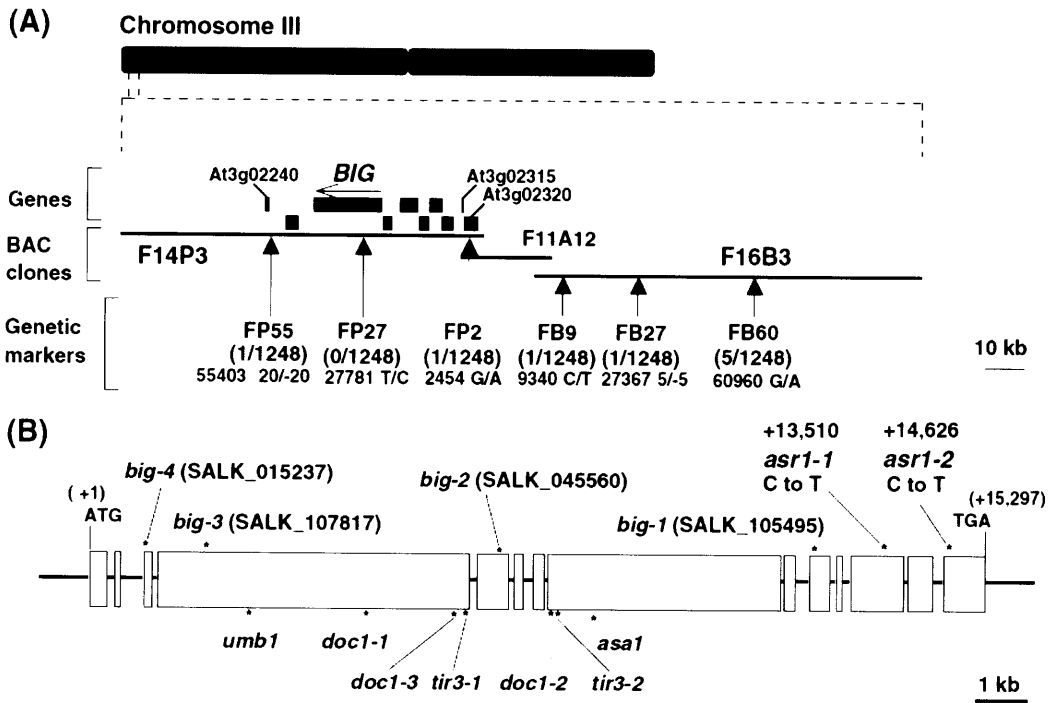


Fig. 1-3. Identification of mutation in *asr1-1* and *asr1-2* mutants. (A) Map of *asr1* mutation locus. The *asr1* mutation locus was mapped to a 53-kb region in the top of chromosome III, between genetic markers FP55 and FP2. In total 1,248 F₂ individuals were analyzed, and the numbers of recombinations were indicated for each genetic marker. The horizontal black bars represent bacterial artificial chromosome (BAC) clones that mapped between FP55 and FB60. The BAC F14P3 contained the gene encoding the *BIG* (open arrow). The direction of the arrow indicates the direction of transcription. (B) Alleles of *big*. Asterisks represent the position of the mutations in *asr1-1*, *asr1-2*, *big-1*, *big-2*, *big-3*, and *big-4* (on the top of the bars) and known reported mutants (beneath the bottom of the bars). Mutations were detected in exons 12 and 14 in *asr1-1* and *asr1-2*. The exon–intron structure is drawn based on data from Kanyuka et al. (2003).

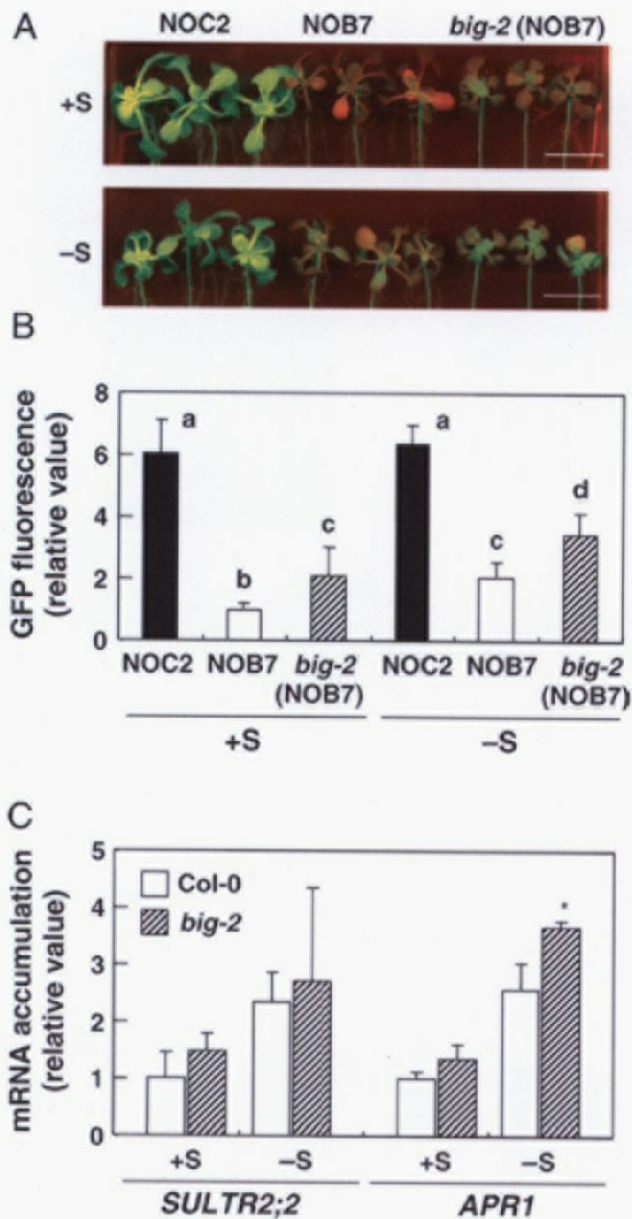


Fig. 1-4. Expression of *GFP*, *SULTR2;2*, and *APR1* in *big-2*. (A) GFP fluorescence of *big-2*(NOB7), which carried the homozygous *big-2* mutation and homozygous *Pro35S::βSRx3::GFP* T-DNA insertion. NOC2, NOB7, and *big-2* (NOB7) were cultivated on the normal medium for 10 days. Then plants were transferred to sulfur-sufficient medium containing 1,500 μM sulfate (+S) or sulfur-deficient medium containing 15 μM sulfate (-S) and cultivated for 4 days. The GFP fluorescence was examined. (B) Semiquantification of GFP fluorescence. Plants were cultivated as described in (A). The intensities of GFP fluorescence (green) were quantified and standardized with the intensities of chlorophyll auto-fluorescence (red). Letters represent the means that were statistically different by Student's *t*-test ($P < 0.05$, $n = 6$); data with the same letters were not significantly different. (C) qPCR analysis. Col-0 wild type and *big-2* were cultivated as in (A). Shoots were sampled and RNA was extracted. The cDNA generated from the extracted RNA was analyzed to quantify the mRNA accumulation of *SULTR2;2* and *APR1*. Asterisks indicate significant changes determined by Student's *t*-test ($P < 0.05$, $n = 3$).

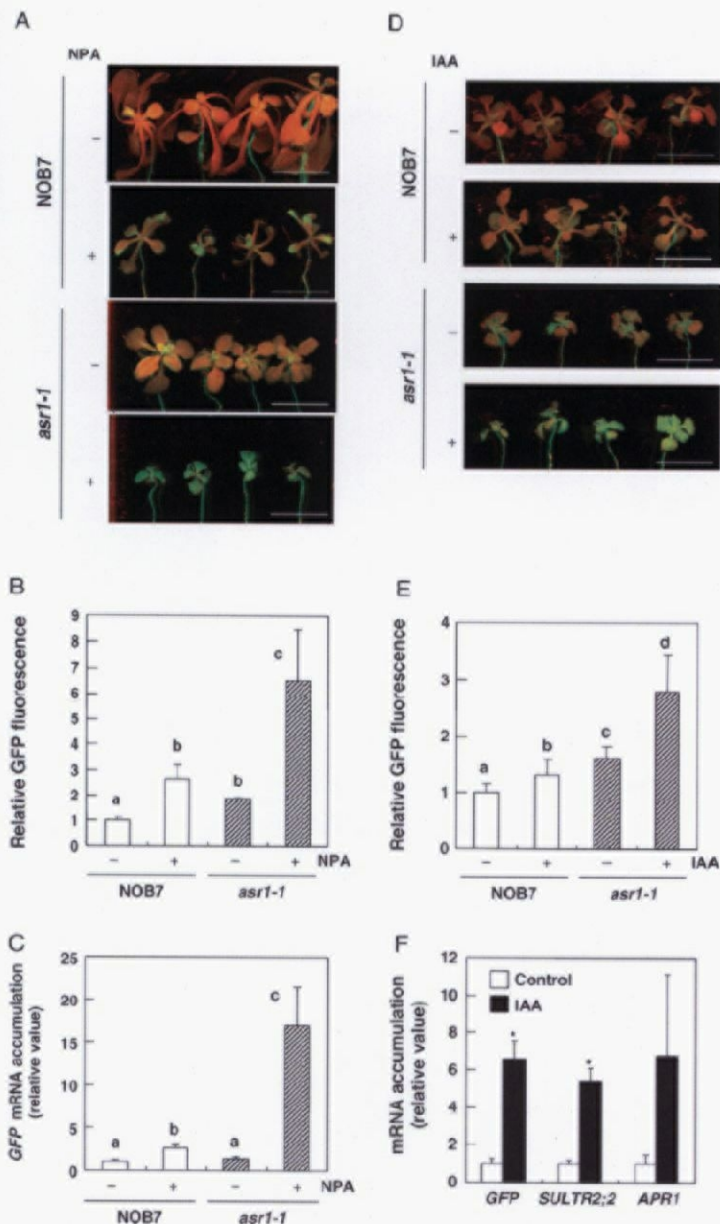


Fig. 1-5. Effects of NPA and IAA application on the expression of *GFP*, *SULTR2;2*, and *APR1*. (A) NOB7 and *asr1-1* were cultivated for 18 days on control medium or medium containing 10 μ M NPA. Fluorescence of plants was observed as shown in Materials and methods; the false image representing fluorescence intensity is shown. (B) Semiquantification of GFP fluorescence of the plants shown in (A). Intensities of GFP fluorescence were quantified as described in Materials and methods. (C) *GFP* mRNA accumulation in plants shown in (A). *GFP* mRNA was quantified by qPCR. (D) NOB7 and *asr1-1* were cultivated for 10 days on the normal medium. Then plants were transferred to control medium or medium containing 10 μ M IAA and cultivated for 4 days. Plants were observed as in (A). (E) Semiquantification of GFP fluorescence of plants shown in (D). (F) Expression of *GFP*, *SULTR2;2*, and *APR1* in NOB7. The mRNA accumulation in shoots of IAA-treated plants of *GFP*, *SULTR2;2*, and *APR1* were quantified by qPCR analysis. Control, NOB7; IAA, NOB7 plants treated with IAA as in (D). Letters and asterisks indicate significant changes determined by Student's *t*-test ($P < 0.05$). Bars = 1 cm.

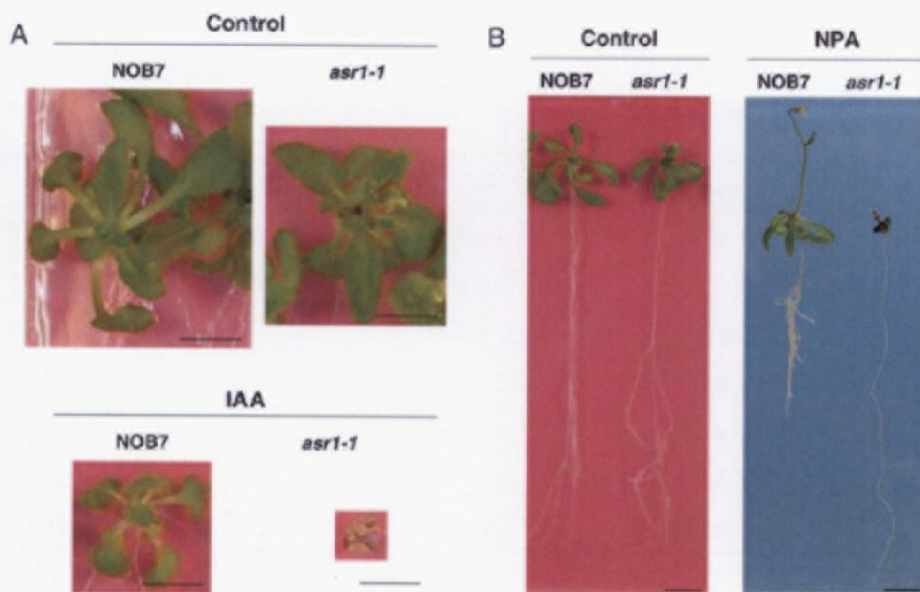


Fig. 1-6. Effects of IAA and NPA treatments on growth of NOB7 and *asr1-1* mutant plants. (A) Growth inhibition by IAA. NOB7 and *asr1-1* were sown on +S medium (upper) or +S medium containing 10 μ M IAA (bottom). After vernalization, plants were incubated for 23 days. Bars = 5 mm. (B) Growth inhibition by NPA. NOB7 and *asr1-1* seeds were sown on standard medium or medium containing 10 μ M NPA. After vernalization, plates were incubated vertically for 23 days. Each line was grown normally on +S medium for 23 days. Bars = 1 cm.

Table 1-1. Morphology of *asr1-1*. The data represent mean and standard deviation (SD) of values for NOB7 or *asr1-1*. Plants were grown for 11 days (for root morphology) or 48 days (for shoot morphology). Asterisks indicate significant differences ($P < 0.05$) between data according to Student's *t* test ($n = 7$ for root morphology; $n = 4$ for shoot morphology).

	NOB7	<i>asr1-1</i>
Length of main roots (cm)	8.2 ± 0.8	5.8 ± 1.3*
Number of lateral roots	15 ± 4	1 ± 2*
Shoot height (cm)	33.3 ± 2.0	15.5 ± 2.5*
Inflorescence number	2 ± 1	7 ± 1*
Siliques	109 ± 14	47 ± 25*
Cauline leaves	21 ± 3	43 ± 12*
Rosette leaves	16 ± 1	46 ± 10*

Table 1-2. Segregation of mutant phenotype in F₂ plants. Backcrossed F₂ plants were counted according to their GFP fluorescence. Mutant lines expressed a higher GFP fluorescence level than the original NOB7. ^a Female x Male. ^b Chi-square values were calculated based on the expected segregation ratio of 3:1. ^c Not significant ($P > 0.05$) based on Student's *t* test.

Crosses	Generation	No. plants tested	Phenotype		Chi-square ^b
			Wild type	Mutant	
Wild type x <i>asr1-1</i> ^a	F2	113	83	30	0.70 ^c
Wild type x <i>asr1-2</i> ^a	F2	99	77	22	0.52 ^c

Table 1-3. Positions of T-DNA insertions in the *BIG* exon of *big* lines. The data indicate the profiles of inserted T-DNAs in *big* lines. Each border sequence of genomic DNA and T-DNA was analyzed. Positions of the flanking sequences are aligned left to right according to the 5' to 3' direction in the *BIG* gene. Numbers indicate the genomic border base positions in the *BIG* exon; "left" and "right" indicate left and right border sequences, respectively, of the T-DNA of pROK2. ^a The 11-bp nucleotide sequence was inserted in the border. ^b The 74-bp nucleotide sequence without significant homology in the database was inserted in the border.

Line	5' exon	T-DNA border 1	T-DNA border 2	3' exon
<i>big-1</i>	12,471 st T	left ^a		
<i>big-2</i>	7,149 th C	left	right ^b	7,159 th A
<i>big-3</i>	1,911 th T	left	left	1,919 th C
<i>big-4</i>	473 rd G	left		

Acknowledgements

asr1 mutants were isolated by Dr. Naoko Ohkama-Ohtsu. *asr1* was also mapped to the chromosome III by Dr. Ohkama. I also received technical assistance by Ms. Kayoko Aizawa in map-based cloning. I would also like to acknowledge the Research Center for Water Environment Technology of the University of Tokyo for facilities, and the National Center for Biotechnology Information (NCBI) and the Salk Institute for providing information and plant materials.

Chapter 2

A protocol for rapid DNA extraction from *Arabidopsis thaliana* for PCR analysis

Abbreviation

PCR, polymerase chain reaction

Introduction

DNA extraction protocols from *Arabidopsis thaliana* usually require several steps, such as boiling, ethanol precipitation, or drying in vacuum. A number of simplified and rapid protocols of DNA extraction for *Arabidopsis* have been reported (Edwards et al. 1991, Wang et al. 1993), however, they still require several steps. Here described is a novel one-step DNA extraction protocol for uses in polymerase chain reaction (PCR).

Results and discussion

In order to develop a one-step protocol, modified concentrations of NaCl and SDS from the original DNA extraction protocol (Edwards et al. 1991) were prepared to avoid inhibition of PCR without significantly affecting the efficiency of DNA extraction. TE and extraction buffers diluted by ten, hundred and thousand folds by TE buffer were used for DNA extraction. One μL of the extracts were subjected to PCR. Extracts with ten fold-diluted buffer gave the most distinct band with an expected molecular weight (Fig. 2-1a). Little or no PCR product was detected from the other dilutions.

Then carried out was extensive PCR test of the extracted DNA solution. PCR reaction was carried out with 23 different sets of primers and bands with expected sizes were detected with all the primer sets (data not shown). Moreover, carried out were total of 236 reactions using independently extracted 67 DNA solutions using 23 different sets of primers and 227 PCR reactions gave bands of expected sizes (96%, data not shown).

The present protocol was also useful for detection of transgene. This experiment was

performed by Ms. Yoko Ide. DNA was extracted from transgenic plants NOB7 (Ohkama et al., 2002) and subjected to PCR reaction using the primer set No.24. A band with expected size was detected (Fig. 2-1b).

Also investigated were amounts of plant tissues required for PCR amplification. DNA was extracted from 1mm² (less than 1 mg) leaf tissue or about 120 µg of petals in fresh weights in 10 µL of the extraction buffer. Appropriate PCR products were observed with these samples as well as with DNA from 1 mg of leaf tissue, suggesting that tissue less than 1 mg in fresh weights are sufficient for PCR analysis (Fig. 2-1c).

The DNA solution was stable for PCR amplification at -20°C at least for one month. Comparison of this method with other rapid methods is shown in Table 2-1. The present protocol is the quickest among the protocols and suitable for PCR analysis. Two novel quick methods were also reported (sucrose prep and touch-and-go methods) after establishment of the present protocol (Berendzen et al. 2005). These methods are accelerating genetic study on plant mechanisms.

Materials and methods

Plant materials

For extensive test of the extracted DNA solution, F₂ plants derived from a cross between *Arabidopsis thaliana* (L.) Heynh. ecotypes Col-0 and Landsberg *erecta* were used. For assay of transgene possession, *Arabidopsis* line NOB7 (Ohkama et al., 2002) was used.

DNA extraction

This protocol uses 1.5-mL centrifuge tubes, plastic rods fit to the 1.5-mL centrifuge tubes to grind samples (such as Pestle for Homogenizer, Azuwan, Osaka, Japan), TE buffer (10 mM Tris-HCl pH 8.0 and 1 mM EDTA) and extraction buffer (200 mM Tris-HCl pH7.5, 250 mM NaCl, 25 mM EDTA and 0.5% SDS; described in Edwards et al. 1991). A piece of rosette leaf (typically 3-5 mg) was placed in a centrifuge tube. 200 µL of extraction buffer which have been diluted 10 fold by TE buffer was added in the tube. The leaves were crushed by pressing them against the walls of the plastic tubes with the rods several times. Crushing was done leaving residues of the tissues visible in the tube as excess crushing of the tissues inhibited subsequent PCR analysis.

PCR amplification and DNA analysis

One µL DNA extract was added to the 20 µL of PCR mixture containing with 10 mM Tris-Cl (pH 7.5), 1.5 mM MgCl₂, 50 mM KCl, 0.5 µM primers, 0.2-1 U Taq DNA polymerase (Roche Applied Science, Mannheim, Germany). Mastercycler gradient (Eppendorf, Hamburg, Germany) was used for the thermal cycling; 2 min at 94°C, followed by 30 cycles of 30 sec at 94°C, 45 sec at 55

°C, 45 sec at 72 °C, and 7 min at 72 °C. For detection of the transgene in NOB7 line, the following cycles were employed; 3 min at 96 °C, followed by 25 cycles of 30 sec at 96 °C, 30 sec at 56 °C, 1 min at 72 °C, and 5 min at 72 °C.

Extensive test of the extracted DNA solution was carried out with 23 sets of primers, which detect polymorphisms in the shorter arm of the chromosome 3. Some of these primers were prepared by Dr. Naoko Ohkama-Ohtsu and technical assistance was made by Ms. Kayoko Aizawa. The sequences of the primers in each set were as follows:

- Primer set 1 · taatccgggttatgggatca/gcctctcagattaaagatgga
- Primer set 2 · cataacccacaaaagagg/ttgtgtgagagattgtcttatactcg
- Primer set 3 · aactcggaccagactcgtga/aattggatcggattcactcg
- Primer set 4 · cggaaacagcttcagtagcc/cggtaagaaaacatagaggaga
- Primer set 5 · tccccctctcgacttgtgt/cactgaaacccactcccttt
- Primer set 6 · ggtggagagacttgattcagga/gagccttggaggatcctactct
- Primer set 7 · aggttctcgcctgagtgaaa/caacttcggccattcctaaa
- Primer set 8 · tcaactcgttggcggtatgta/caatgctccttatgcctgg
- Primer set 9 · tcttaatctttttatttccgatgaca/tcaaaagtccacttctcccttt
- Primer set 10 · tgaagccaagtatccactcaa/tgctttctttgtggaggaca
- Primer set 11 · tctgagcatcctcgtttgt/gcttcaaactcctctgtcgg
- Primer set 12 · gtctccccgttgggaataat/ttcaactcagcggagaacctt
- Primer set 13 · tagtcaaagcccgaagaaa/tcccctaaggaagagcaggt
- Primer set 14 · ttctggttgctcacatggtt/cttccaccacggataagca
- Primer set 15 · aaatggctgctcttgattacc/gccttaaccgtggttgaaaa
- Primer set 16 · tgaaccaaagacaggggatt/cttggggttctctcttggg
- Primer set 17 · aaatgtggcgatcgtgaagt/ctccgtagcagaaaccacg
- Primer set 18 · tcatccgggtaaaaagcatc/gatccattccagcattgtca
- Primer set 19 · caaatccatctccgcgatac/aatgggaattttcaacggaa
- Primer set 20 · ttgcaatcctgcttcacaac/atccactgcatcccttagga
- Primer set 21 · gatacttggcggattgcta/cccgtaaaatgacggtact
- Primer set 22 · cttgaaccgaagatgggaga/tccctgcataagatgccttg
- Primer set 23 · tgcagcagaaggggtagtct/atctcccaggaatccagtt

In addition, primer set No.24 (NOBf:gctaaagggccaagtcca/NOBr:actcagcactcttacgcgt and Bin4:taaaaacgtccgcaatgtgt, Ohkama et al., 2002) was used for detection of the transgene in NOB7 transgenic plants. NOBf and NOBr are derived from upstream and downstream adjacent sequence of the transgene, respectively, and Bin4 is from sequence in the transgene.

PCR products (5-20 µL) were analyzed using 1.4 % agarose gel electrophoresis, stained with ethidium bromide and visualized with UV light.

References

- Berendzen K, Searle I, Ravenscroft D, Koncz C, Batschauer A, Coupland G, Somssich IE, Ülker B (2005) A rapid and versatile combined DNA/RNA extraction protocol and its application to the analysis of a novel DNA marker set polymorphic between *Arabidopsis thaliana* ecotypes Col-0 and Landsberg *erecta*. *Plant Methods* 1: 4
- Edwards K, Johnstone C, Thompson C (1991) A simple and rapid method for the preparation of plant genomic DNA for PCR analysis. *Nucl Acid Res* 19: 1349
- Ohkama N, Goto DB, Fujiwara T, Naito S (2002) Differential tissue-specific response to sulfate and methionine of a soybean seed storage protein promoter region in transgenic *Arabidopsis*. *Plant Cell Physiol* 43: 1266-1275
- Wang H, Qi M, Cutler AJ (1993) A simple method of preparing plant samples for PCR. *Nucl Acid Res* 21: 4153-4154

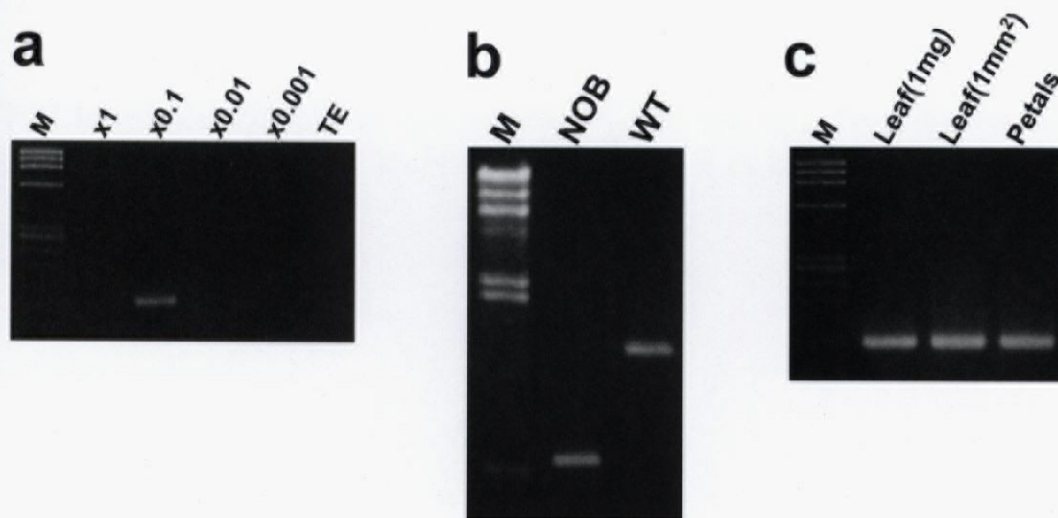


Fig. 2-1. Electrophoresis of PCR products. (a) Effect of dilution of the extraction buffer on PCR amplification. Original buffer (x1) and ten- (x0.1), hundred- (x0.01) and thousand- (x0.001) folds diluted buffers were tested together with the TE buffer. Primer set 1 was used for amplification which should produce 118 bp DNA. M: molecular weight marker ϕ X174-*Hae*III. (b) Assay of transgene possession. NOB7 and wild-type plants were assayed. M: λ -*Hind*III. The transgene of NOB7 plants is located between the target sites of NOBf (left primer) and NOBr (right primer) on chromosome V. The target site of Bin4 (right primer) is on NOB insert. NOB transgenic plant gives 677bp PCR product primed by NOBf and Bin4, and wild-type plant gives 1337 bp PCR product primed by NOBf and NOBr. (c) PCR product of DNA micro-scale extraction. Normal-scale extraction was carried out from 1 mg leaf tissue and micro-scale extractions from about 1 mm² leaf tissue and 2 petals. Primer set 3 was used for amplification which should amplify DNA of 116 bps. M: molecular weight marker ϕ X174-*Hae*III.

Table 2-1. Comparison of rapid methods of DNA extraction from *Arabidopsis*. Manipulation times were calculated as a sum of manipulation time for each step: the time was hypothesized as 30 seconds for every pipetting and homogenization.

	Number of solutions used	Manipuration time	Minimum sample amount
Edwards et al. 1991	3	> 1 hr.	No data
Wang et al. 1993	2	2.5 min.	No data
Present method	1	1 min.	~ 120 μ g

Acknowledgements

PCR detection of T-DNA insert was performed by Ms. Yoko Ide. Some primers were designed by Dr. Naoko Ohkama-Ohtsu. Ms. Kayoko Aizawa gave technical assistance in PCR analysis.